Structural trends for celestite (SrSO$_4$), anglesite (PbSO$_4$), and barite (BaSO$_4$): Confirmation of expected variations within the SO$_4$ groups

SYTLE M. ANTAO*

Department of Geoscience, University of Calgary, Calgary, Alberta T2N 1N4, Canada

ABSTRACT

The crystal structures of the isostructural orthorhombic sulfates celestite (SrSO$_4$), anglesite (PbSO$_4$), and barite (BaSO$_4$) were refined by Rietveld methods using synchrotron high-resolution powder X-ray diffraction (HRPXRD) data. Their structural model was refined in space group *Pbnm*. The unit-cell parameters are $a = 6.87032(3)$, $b = 8.36030(5)$, $c = 5.34732(1)$ Å, and $V = 307.139(3)$ Å^3 for SrSO$_4$; $a = 6.95802(1)$, $b = 8.48024(3)$, $c = 5.39754(1)$ Å, and $V = 318.486(1)$ Å^3 for PbSO$_4$; and $a = 7.15505(1)$, $b = 8.88101(3)$, $c = 5.45447(1)$ Å, and $V = 346.599(1)$ Å^3 for BaSO$_4$. The average <M-O> [12] distances are 2.827(1), 2.865(1), and 2.953(1) Å for SrSO$_4$, PbSO$_4$, and BaSO$_4$, respectively, and their corresponding average <S-O> [4] distances are 1.480(1), 1.477(3), and 1.471(1) Å. The geometrical features of the SO$_4$ and MO$_{12}$ polyhedra become more symmetrical from SrSO$_4$ to BaSO$_4$. Across the series, the a, b, and c parameters vary non-linearly with increasing V. The radii of the M^{2+} cations, r_M, <M-O> [12], and <S-O> [4] distances vary linearly with V. These structural trends arise from the effective size of the M^{2+} cation (r_M: Sr < Pb < Ba) that is coordinated to 12 O atoms.

Keywords: Celestite, SrSO$_4$, anglesite, PbSO$_4$, barite, BaSO$_4$, Rietveld refinement, synchrotron high-resolution powder X-ray diffraction (HRPXRD), crystal structure

INTRODUCTION

Celestite (SrSO$_4$) and barite (BaSO$_4$) occur in hydrothermal veins and as secondary minerals in sedimentary environments. They are the main commercial sources of strontium and barium. Anglesite (PbSO$_4$), a minor ore of lead, typically occurs in the oxidized portion of hydrothermal lead deposits as an alteration product of galena and also as a primary mineral in some low-temperature oxidized hydrothermal deposits.

The crystal structures of isostructural celestite, anglesite, and barite were determined by James and Wood (1925). Sahl (1963) refined the structural model for anglesite and barite. The barite structure was also refined by Colville and Staudhammer (1967). The structure of celestite was refined by Garske and Peacor (1965) and Hawthorne and Ferguson (1975). The structure of a Ba-rich celestite is also available (Brigatti et al. 1997). The structure of all three minerals was refined by Miyake et al. (1978) and Jacobsen et al. (1998) to determine structural trends that are expected across the series. The structure refinements were carried out in space group *Pbnm*. The main structural features of the orthorhombic sulfates, SrSO$_4$, PbSO$_4$, and BaSO$_4$, listed with increasing size of the M^{2+} cation, are SO$_4$ and MO$_{12}$ polyhedra that share edges (Fig. 1).

Miyake et al. (1978) indicated a possible systematic variation in the SO$_4$ tetrahedron with field strength of the M^{2+} cation across the series, but their SO$_4$ geometry was statistically identical (Jacobsen et al. 1998). Heavy M^{2+} cation makes it difficult to determine the atom positions of light elements with high precision

using conventional X-ray diffraction because of strong absorption effects and the small relative contribution of the oxygen atoms to the total scattering. Consequently, Jacobsen et al. (1998) used single-crystal and high-intensity rotating anode Mo X-ray source data to refine the structure of these isostructural minerals. They concluded that the average <M-O> [12] distance increases linearly with increasing cell volume, but the SO$_4$ behaves as a rigid group with an average <S-O> [4] distance of 1.476 Å, which is constant across the series. Hawthorne and Ferguson (1975) and Hill (1977) reported that the SO$_4$ groups in all three minerals display identical geometries, and the M cation is [l2]-coordinated to O atoms because of bond-strength sums.

Although previous studies indicate that the M^{2+} cations have no effect on the shape or size of the SO$_4$ tetrahedron (e.g., Jacobsen et al. 1998), the M^{2+} cations have different sizes and effective charge, so systematic variation in the geometry of the SO$_4$ group is expected. The purpose of this study is to examine the structural trends for SrSO$_4$, PbSO$_4$, and BaSO$_4$. Using high-resolution powder X-ray diffraction (HRPXRD), this study shows that the geometry of the SO$_4$ group varies in a systematic and expected manner.

EXPERIMENTAL METHODS

Sample characterization

The celestite sample is from Saxony, Ngar Majunga, Madagascar (UC15824). The barite sample is from Elk Creek, South Dakota. The synthetic PbSO$_4$ sample was obtained as high-purity (99.995%) reagent grade powder from Aldrich and no impurity phase was observed in the HRPXRD trace.

The celestite and barite samples were analyzed using a JEOL JXA-8200 electron microprobe and its standard operating program on a Solaris platform.
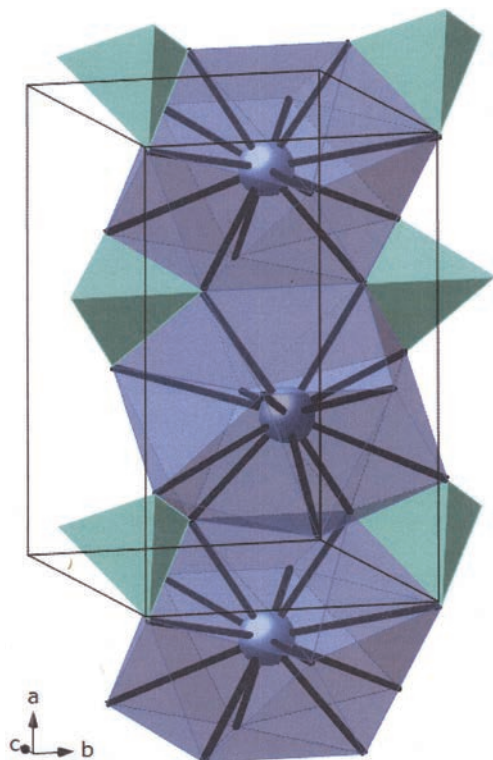
FIGURE 1. Projection of the $SrSO_4$ structure (based on data from this study). The Sr atom is coordinated to 12 O atoms of six different SO_4 groups. The SO_4 and SrO_{12} polyhedra share edges. (Color online.)

The wavelength-dispersive operating conditions were 15 kV accelerating voltage, 10 nA beam current, a beam diameter of 5 μm, and using various standards [e.g., fluorapatite (Ca$K\alpha$, P$K\alpha$, F$K\alpha$), barite (Ba$K\alpha$, S$K\alpha$), hornblende (Fe$K\alpha$, Mg$K\alpha$), scapolite (Cl$K\alpha$), strontianite (Sr$K\alpha$), and rhodonite (Mn$K\alpha$)]. The crystals are homogeneous based on optical observations and electron microprobe analyses of 10 spots for each sample. Representative chemical compositions of the samples are given (Table 1). The MSO_4 formula was used in the structure refinements as the samples are quite pure, as indicated by the chemical analyses.

Synchrotron high-resolution powder X-ray diffraction (HRPXRD)

The samples were studied by HRPXRD experiments that were performed at beamline 11-BM, Advanced Photon Source (APS), Argonne National Laboratory (ANL). Each sample was crushed to a fine powder using an agate mortar and pestle. The crushed samples were loaded into Kapton capillaries (0.8 mm internal diameter) and rotated during the experiment at a rate of 90 rotations per second. The data were collected at 23 °C to a maximum 2θ of about 43° with a step size of 0.001° and a step time of 0.1 s per step. The HRPXRD traces were collected with 12 silicon (111) crystal analyzers that increase detector efficiency, reduce the angular range to be scanned, and allow rapid acquisition of data. A silicon (NIST 640c) and alumina (NIST 676a) standard (ratio of ⅓ Si: ⅔ Al₂O₃) was used to calibrate the instrument and refine the wavelength used in the experiment (see Table 2). Additional details of the experimental setup are given elsewhere (Antao et al. 2008; Lee et al. 2008; Wang et al. 2008).

Rietveld structure refinements

The HRPXRD data were analyzed by the Rietveld method (Rietveld 1969), as implemented in the GSAS program (Larson and Von Dreele 2000), and using the EXPGUI interface (Toby 2001). Scattering curves for neutral atoms were used. The starting atom coordinates, cell parameters, and space group, *Pbnm*, were taken from Jacobsen et al. (1998). The background was modeled using a Chebyschev polynomial (12 terms). The reflection-peak profiles were fitted using type-3 profile

TABLE 1. Electron microprobe analyses (EMPA) for celestite and barite

	Celestite Madagascar wt% oxide	Barite South Dakota wt% oxide
CaO	0.01(1)†	0.03(4)
MgO	0.00(1)	0.03(1)
FeO	0.02(1)	0.00(2)
SrO	54.83(7)	0.3(1)
BaO	0.06(4)	64.9(5)
F	0.02(3)	0.00(1)
Cl	0.07(3)	0.00(1)
SO₃	45.06(5)	34.6(4)
Total	100.07	99.76
	apfu*	
Ca	0.000(1)	0.001(1)
Mg	0.000(1)	0.002(1)
Fe	0.001(1)	0.000(1)
Sr	0.966(5)	0.007(3)
Ba	0.001(1)	0.985(6)
F	0.002(3)	0.000(2)
Cl	0.004(1)	0.000(1)
S	1.027(6)	1.005(7)

Notes: Formula for celestite is $[Sr_{0.966}Fe_{0.001}Ba_{0.001}]_{\Sigma0.97}(SO_4)_{1.03}$. Formula for barite is $[Ba_{0.985}Sr_{0.007}Mg_{0.002}Ca_{0.001}]_{\Sigma1.00}(SO_4)_{1.01}$.
* The values of atoms per formula unit (apfu) are based on sum of cations and anions (except O) = 2.
† The estimated standard deviations in brackets are based on analyses of 10 spots for each sample and are given to the last two decimal places for the oxides and three for the apfu.

in the GSAS program. Full-matrix least-squares refinements were carried out by varying the parameters in the following sequence: a scale factor, cell parameters, atom coordinates, and isotropic displacement parameters. Toward the end of the refinement, all the parameters were allowed to vary simultaneously, and the refinement proceeded to convergence. The fitted HRPXRD traces are shown in Figure 2.

The cell parameters and the Rietveld refinement statistics are listed in Table 2. Atom coordinates and isotropic displacement parameters are given in Table 3. Bond distances and angles are given in Table 4.

RESULTS AND DISCUSSION

Structure of SrSO₄, PbSO₄, and BaSO₄

The three isostructural minerals have SO_4 and MO_{12} polyhedra that share edges (Fig. 1). The M^{2+} (=Sr, Pb, or Ba) cation is coordinated to 12 O atoms (Hawthorne and Ferguson 1975; Hill 1977; Jacobsen et al. 1998; Brigatti et al. 1997). However, there are ranges of various M-O distances, so the nearest O atoms can be grouped into 8, 10, or 12 distances (Table 4).

Structural trends

The radii, r_M, of the 12-coordinated M^{2+} cations (Shannon 1976) and the *a*, *b*, *c* unit-cell parameters are plotted against the

TABLE 2. Cell parameters and Rietveld refinement statistics for the orthorhombic sulfates

	Celestite SrSO₄ Madagascar	Anglesite PbSO₄ synthetic	Barite BaSO₄ South Dakota
a (Å)	6.87032(3)	6.95802(1)	7.15505(1)
b (Å)	8.36030(5)	8.48024(3)	8.88101(3)
c (Å)	5.34732(1)	5.39754(1)	5.45447(1)
V (Å³)	307.139(3)	318.486(1)	346.599(1)
λ (Å)	0.41220(2)	0.41399(2)	0.41416(2)
R (*F²*)	0.0415	0.0756	0.0271
N_obs	1084	1036	1219
2θ range	3.5–43°	3.5–43°	3.5–43°

*R (*F²*) = R-structure factor based on observed and calculated structure amplitudes = $[\Sigma(F_o^2 - F_c^2)/\Sigma(F_o^2)]^{1/2}$. Space group is *Pbnm*; the number of formula units per cell, *Z* = 4. The number of data points for each trace is 39 499.
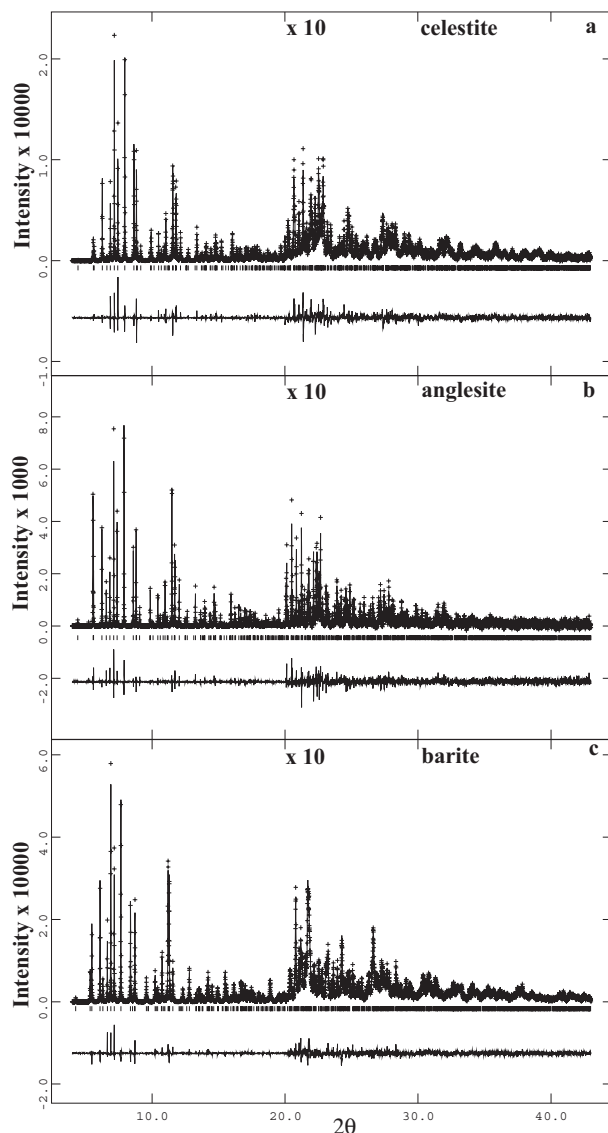
FIGURE 2. Comparison of the HRPXRD traces for $SrSO_4$, $PbSO_4$, and $BaSO_4$, together with the calculated (continuous line) and observed (crosses) profiles. The difference curve ($I_{obs} - I_{calc}$) is shown at the bottom. The short vertical lines indicate allowed reflection positions. The intensities that are above 20 °2θ are scaled by a factor of 10. The FWHM for the (021) reflection in $PbSO_4$ is 0.010°, $SrSO_4$ is 0.017°, and $BaSO_4$ is 0.018°.

TABLE 3. Atom coordinates and isotropic displacement parameters (x100 Å²) for the orthorhombic sulfates

		Celestite $SrSO_4$ Madagascar	Anglesite $PbSO_4$ synthetic	Barite $BaSO_4$ South Dakota
M	x	0.15826(7)	0.16722(6)	0.15803(3)
	y	0.18405(4)	0.18782(4)	0.18445(2)
	z	0.25	0.25	0.25
	U	1.01(1)	1.90(1)	1.120(4)
S	x	0.1843(2)	0.1837(3)	0.19161(8)
	y	0.4388(1)	0.4362(3)	0.43803(8)
	z	0.75	0.75	0.75
	U	0.89(3)	0.82(5)	0.61(2)
O1	x	0.0933(3)	0.0953(8)	0.1081(2)
	y	0.5952(3)	0.5921(7)	0.5874(2)
	z	0.75	0.75	0.75
	U	1.68(8)	2.05(17)	1.78(5)
O2	x	0.0401(4)	0.0474(8)	0.0480(2)
	y	0.3067(4)	0.3072(7)	0.3187(2)
	z	0.75	0.75	0.75
	U	1.55(7)	2.33(16)	1.04(4)
O3	x	0.3120(3)	0.3090(6)	0.3101(2)
	y	0.4223(2)	0.4191(4)	0.4200(1)
	z	0.9743(3)	0.9747(6)	0.9695(2)
	U	1.12(5)	1.52(1)	0.86(3)

TABLE 4. Selected interatomic distances (Å) and angles (°) for the orthorhombic sulfates

Bonds/angles		Celestite $SrSO_4$ Madagascar	Anglesite $PbSO_4$ synthetic	Barite $BaSO_4$ South Dakota
M-O1	x1	2.528(2)	2.612(5)	2.781(2)
M-O2	x1	2.624(3)	2.645(6)	2.790(2)
M-O3	x2	2.694(2)	2.651(4)	2.811(1)
M-O3	x2	2.646(2)	2.726(4)	2.812(1)
M-O3	x2	2.809(2)	2.917(4)	2.914(1)
<M-O> [8]		2.681(2)	2.731(2)	2.831(1)
M-O2	x2	2.976(1)	3.001(3)	3.079(1)
<M-O> [10]		2.740(1)	2.785(1)	2.880(1)
M-O1	x2	3.258(1)	3.267(3)	3.314(1)
<M-O> [12]		2.827(1)	2.865(1)	2.953(1)
S-O1	x1	1.450(2)	1.458(6)	1.455(2)
S-O2	x1	1.484(3)	1.449(6)	1.476(2)
S-O3	x2	1.492(2)	1.500(4)	1.476(1)
<S-O> [4]		1.480(1)	1.477(3)	1.471(1)
O1-S-O2	x1	112.5(2)	114.1(4)	111.66(9)
O1-S-O3	x2	109.7(1)	109.5(2)	109.56(7)
O2-S-O3	x2	108.9(1)	107.9(2)	108.78(6)
O3-S-O3	x1	107.0(1)	107.9(3)	108.46(9)
<O-S-O> [6]		109.5(1)	109.4(1)	109.46(3)

cell volume, V (Fig. 3). Non-linear trends are observed. The r_M increases linearly with increasing V (Fig. 3d).

The unit-cell parameters for the isostructural sulfates are in good agreement with those obtained previously (Hawthorne and Ferguson 1975; Miyake et al. 1978; Jacobsen et al. 1998; Brigatti et al. 1997; Fig. 3; Table 2). The close agreement of the cell data with previous studies indicate that the minerals occur as nearly pure end-members without significant substitution by other cations. The Ba-rich celestite data from Brigatti et al. (1997) are on the expected trends because of the incorporation of Ba

atoms. The increase in cell parameters arises from the increase in average size of the M^{2+} cation.

The average <M-O> [12] distance increases linearly with increasing V and they agree with previous results (Fig. 4). The data from this study shows that the MO_{12} polyhedron becomes less distorted with increase in size of the M^{2+} cation. That is, the individual M-O distances are closer to the average <M-O> distance in $BaSO_4$ than in $SrSO_4$ (Table 4).

The interesting aspect of this study is the geometry of the SO_4 group. The geometrical features of the SO_4 group are plotted against V and radii, r_M, of the 12-coordinated M^{2+} cation (Fig. 5). The average <S-O> distance decreases linearly with increasing V (Fig. 5a) and increasing r_M (Fig. 5c). The average <O-S-O> angle increases slightly with increasing V (Fig. 5b). The geometry of the SO_4 group becomes more symmetrical (individual S-O distances and O-S-O angle are closer to the average values) from $SrSO_4$ to $BaSO_4$. Therefore, the celestite structure is most distorted and the barite structure is least distorted in terms of the geometry of
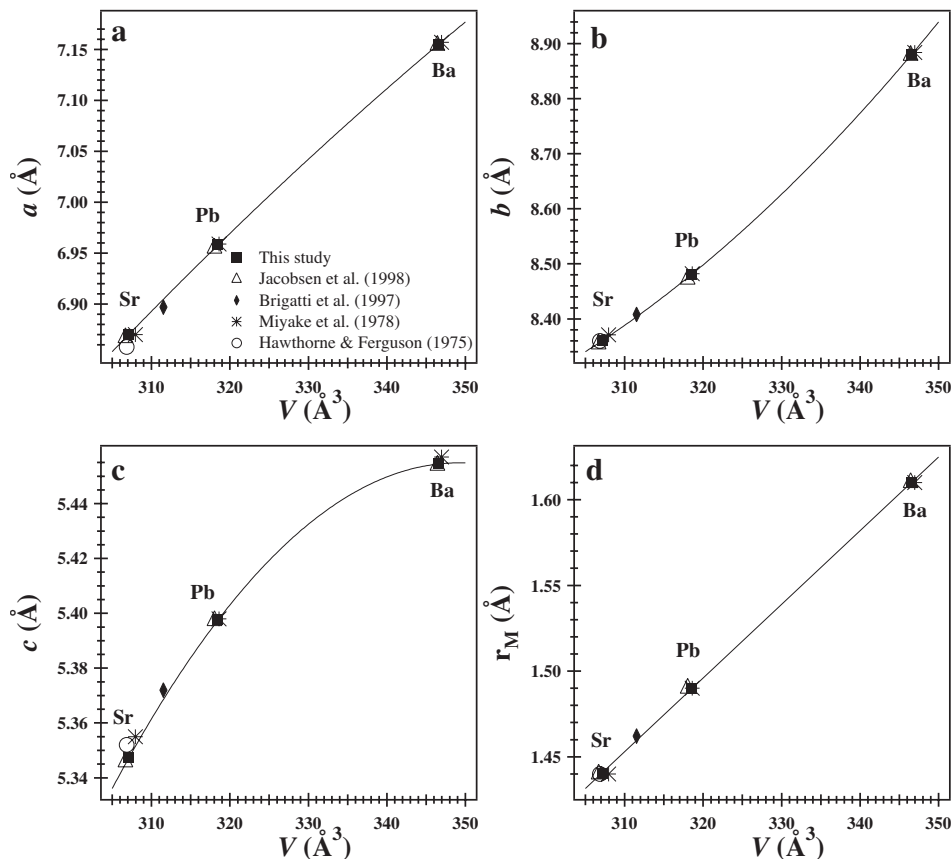
FIGURE 3. The a, b, c unit-cell parameters and the radii, r$_M$, of the [12]-coordinated M^{2+} cation vs. volume, V. The a, b, and c parameters vary non-linearly (**a**, **b**, **c**), and the r$_M$ varies linearly with V (**d**). Data from Jacobsen et al. (1998), Brigatti et al. (1997), Miyake et al. (1978), and Hawthorne and Ferguson (1975) are included for comparison in Figures 3, 4, and 5. The least-squares fitted trend lines shown in Figures 3 to 5 are based only on data from this study. Error bars are smaller than the symbols in Figures 3 and 4.

the SO$_4$ and MO$_{12}$ polyhedra. The structural parameters for the three minerals are correlated with effective size of the M^{2+} cation. In SrSO$_4$, the small Sr^{2+} cation forms a short average <Sr-O> distance, so the charge on the O atoms is less and the average <S-O> distance is longer. In BaSO$_4$, the large Ba^{2+} cation forms a longer average <Ba-O> distance, so the charge on the O atoms is more and the average <S-O> distance is shorter (Figs. 4 and 5).

The geometry of the SO$_4$ group obtained by the single-crystal method shows considerable variations (Fig. 5). Data from Miyake et al. (1978) do not follow any general trend. Data from Jacobsen et al. (1998) indicate that the average <S-O> distance is constant across the series (Figs. 5a and 5c), and that SO$_4$ behaves as a rigid group with a fixed <S-O> distance, which is not supported by the present results.

The structural trends show that cell parameters and average <M-O> [12] distances are easily obtained with X-ray diffraction using either single-crystal or powder samples (Figs. 3 and 4). This is not the case for the geometry of the SO$_4$ group because of the light O^{2-} and S^{6+} ions in the presence of heavy M^{2+} cations (Fig. 5). Problems arise because light atoms contribute little to the total scattering effect and absorption is associated with heavy M^{2+} cations; such problems appear to be more
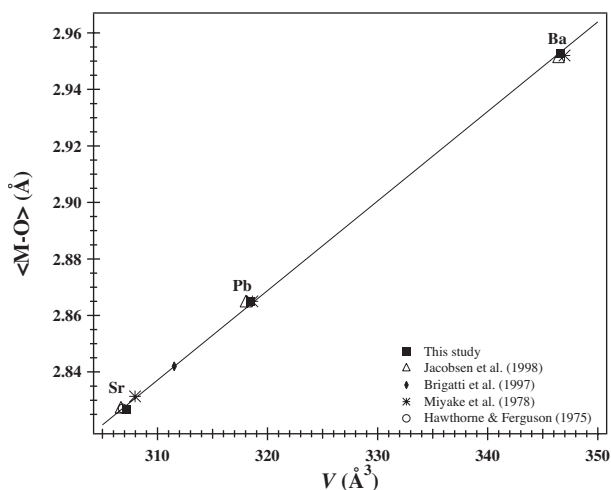
FIGURE 4. Linear increase in average <M-O> [12] distance with increasing volume, V. Data from this study and the literature agree quite well. The equation for the straight line and the goodness-of-fit are <M-O> $= 0.0031V + 1.8870$ and R$^2 = 0.9975$, respectively. The Ba-rich celestite data point from Brigatti et al. (1997) falls on the trend line shown.
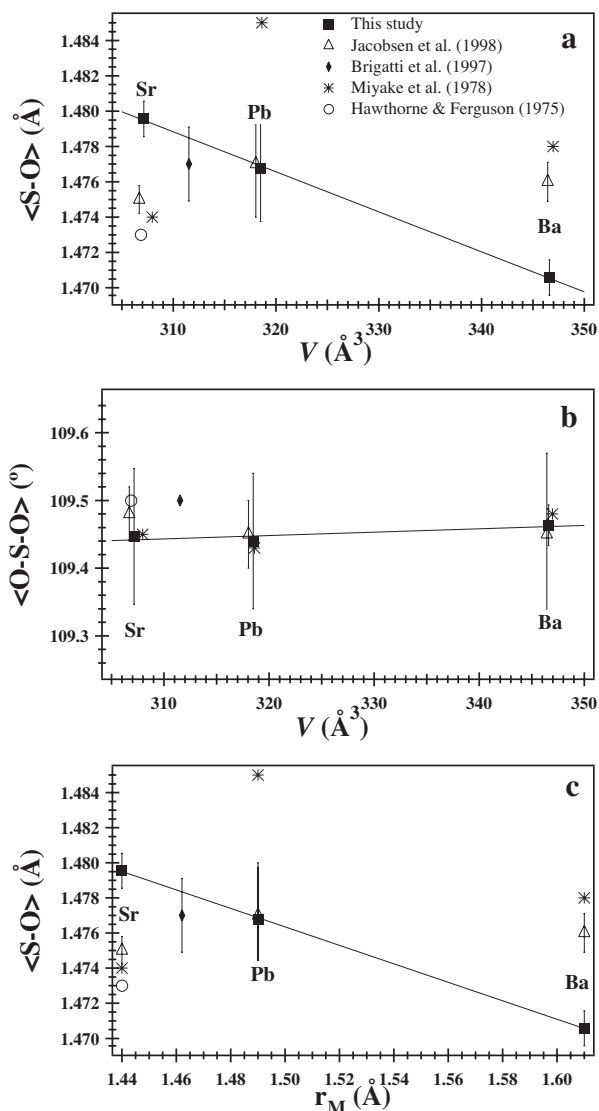
FIGURE 5. Linear variations of (**a**) average <S-O> distance vs. V, (**b**) average <O-S-O> angle vs. V, and (**c**) average <S-O> distance vs. radii, r_M, of [12]-coordinated M^{2+} cation.

pronounced for conventional X-ray diffraction compared to synchrotron diffraction data.

This study shows that in the isostructural sulfate minerals, several well-defined structural trends occur; in particular, the geometry of the SO_4 group changes in a regular manner, as expected. Similar results were obtained for the orthorhombic carbonates (Antao and Hassan 2009), where the geometry of the CO_3 group changes in a regular manner. In addition, the geometry for the SiO_4 group in framework silicates also changes in a regular manner (Antao et al. 2008). Such expected structural trends were not previously observed. Based on the structural trends observed in this study, the average <S-O> distance in anhydrite [$CaSO_4$; <S-O> = 1.4848(3) Å] is expected to be longer than that in celestite [$SrSO_4$; <S-O> = 1.480(1) Å], which

was recently confirmed (Antao 2011). In addition, the average <S-O> distance in gypsum ($CaSO_4 \cdot 2H_2O$) is expected to be a little longer than that in anhydrite.

REFERENCES CITED

Antao, S.M. (2011) Crystal-structure analysis of four mineral samples of anhydrite, CaSO₄, using synchrotron high-resolution powder X-ray diffraction data. Powder Diffraction, 26, 326–330.

Antao, S.M. and Hassan, I. (2009) The orthorhombic structure of CaCO₃, SrCO₃, PbCO₃, and BaCO₃: linear structural trends. Canadian Mineralogist, 47, 1245–1255.

Antao, S.M., Hassan, I., Wang, J., Lee, P.L., and Toby, B.H. (2008) State-of-the-art high-resolution powder X-ray diffraction (HRPXRD) illustrated with Rietveld structure refinement of quartz, sodalite, tremolite, and meionite. Canadian Mineralogist, 46, 1501–1509.

Brigatti, M.F., Galli, E., and Medici, L. (1997) Ba-rich celestine: new data and crystal structure refinement. Mineralogical Magazine, 61, 447–451.

Colville, A.A. and Staudhammer, K. (1967) A refinement of the structure of barite. American Mineralogist, 52, 1877–1880.

Garske, D. and Peacor, D.R. (1965) Refinement of the structure of celestite SrSO₄. Zeitschrift für Kristallographie, 121, 204–210.

Hawthorne, F.C. and Ferguson, R.B. (1975) Anhydrous sulphates. I. Refinement of the crystal structure of celestite with an appendix on the structure of thenardite. Canadian Mineralogist, 13, 181–187.

Hill, R.J. (1977) A further refinement of the barite structure. Canadian Mineralogist, 15, 522–526.

Jacobsen, S.D., Smyth, J.R., Swope, R.J., and Downs, R.T. (1998) Rigid-body character of the SO₄ groups in celestine, anglesite and barite. Canadian Mineralogist, 36, 1053–1060.

James, R.W. and Wood, W.A. (1925) The crystal structure of barytes, celstine and anglesite. Proceedings of the Royal Society of London, 109, 598–620.

Larson, A.C. and Von Dreele, R.B. (2000) General Structure Analysis System (GSAS). Los Alamos National Laboratory Report LAUR 86-748.

Lee, P.L., Shu, D., Ramanathan, M., Preissner, C., Wang, J., Beno, M.A., Von Dreele, R.B., Ribaud, L., Kurtz, C., Antao, S.M., Jiao, X., and Toby, B.H. (2008) A twelve-analyzer detector system for high-resolution powder diffraction. Journal of Synchrotron Radiation, 15, 427–432.

Miyake, M., Minato, I., Morikawa, H., and Iwai, S.-I (1978) Crystal structures and sulphate force constants of barite, celestite, and anglesite. American Mineralogist, 63, 506–510.

Rietveld, H.M. (1969) A profile refinement method for nuclear and magnetic structures. Journal of Applied Crystallography, 2, 65–71.

Sahl, K. (1963) Die Verfeinerung der Kristallstrukturen von PbCl₂ (Cotunnit), BaCl₂, PbSO₄ (Anglesit) und BaSO₄ (Baryt). Beiträge zur Mineralogie und Petrographie, 9, 111–132.

Shannon, R.D. (1976) Revised effective ionic radii and systematic studies of interatomic distances in halides and chalcogenides. Acta Crystallographica, A32, 751–767.

Toby, B.H. (2001) EXPGUI, a graphical user interface for GSAS. Journal of Applied Crystallography, 34, 210–213.

Wang, J., Toby, B.H., Lee, P.L., Ribaud, L., Antao, S.M., Kurtz, C., Ramanathan, M., Von Dreele, R.B., and Beno, M.A. (2008) A dedicated powder diffraction beamline at the advanced photon source: commissioning and early operational results. Review of Scientific Instruments, 79, 085105.